



Observations of cold antihydrogen

J.N. Tan ^a, N.S. Bowden ^a, G. Gabrielse ^{a,*}, P. Oxley ^a, A. Speck ^a, C.H. Storry ^a,
M. Wessels ^a, D. Grzonka ^b, W. Oelert ^b, G. Schepers ^b, T. Sefzick ^b, J. Walz ^c,
H. Pittner ^d, T.W. Hänsch ^{d,e}, E.A. Hessels ^f

ATRAP Collaboration

^a Department of Physics, Harvard University, 17 Oxford Street, Cambridge, MA 02138, USA

^b IKP, Forschungszentrum Jülich GmbH, 52425 Jülich, Germany

^c CERN, 1211 Geneva 23, Switzerland

^d Max-Planck-Institut für Quantenoptik, Hans-Kopfermann-Strasse 1, 85748 Garching, Germany

^e Ludwig-Maximilians-Universität München, Schellingstrasse 4/III, 80799 München, Germany

^f Department of Physics and Astronomy, York University, Toronto, Ontario, Canada M3J 1P3

Abstract

ATRAP's e^+ cooling of \bar{p} in a nested Penning trap has led to reports of cold \bar{H} produced during such cooling by the ATHENA and ATRAP collaborations. To observe \bar{H} , ATHENA uses coincident annihilation detection and ATRAP uses field ionization followed by \bar{p} storage. Advantages of ATRAP's field ionization method include the complete absence of any background events, and the first way to measure which \bar{H} states are produced. ATRAP enhances the \bar{H} production rate by driving many cycles of e^+ cooling in the nested trap, with more \bar{H} counted in an hour than the sum of all the other antimatter atoms ever reported. The number of \bar{H} counted per incident high energy \bar{p} is also higher than ever observed. The first measured distribution of \bar{H} states is made using a pre-ionizing electric field between separated production and detection regions. The high rate and the high Rydberg states suggest that the \bar{H} is formed via three-body recombination, as expected.

© 2003 Elsevier B.V. All rights reserved.

PACS: 36.10.-k; 52.20.-j

Keywords: Antihydrogen; Nested Penning trap; Positron cooling; Recombination in cold plasma; Rydberg atom; Field ionization

1. Introduction

Fifteen years ago emerging techniques (in particular, the capture and cooling of the first \bar{p} by the TRAP Collaboration) encouraged the thought of

using stored antiprotons to form \bar{H} that was cold enough to confine in a magnetic trap for precise laser spectroscopy. As futuristic as it seemed, the goal of cold antihydrogen production and storage for spectroscopic tests of fundamental symmetries was set forth in print [1]. In the intervening years, our TRAP Collaboration developed the techniques to slow, capture, cool and stack cold \bar{p} at 4 K [2,3], an energy more than 10^{10} times lower than any other source. These techniques, developed at

* Corresponding author.

E-mail address: gabrielse@physics.harvard.edu (G. Gabrielse).

LEAR (the low energy antiproton ring), made possible a precise comparison of the charge-to-mass ratios of the \bar{p} and p with an accuracy of 90 ppt [2], the most precise test of CPT invariance with baryons by orders of magnitude. Meanwhile, some high velocity \bar{H} were observed [4,5], but these cannot be easily used for precise studies.

Although LEAR had to be decommissioned, a new CERN storage ring (the antiproton decelerator, or AD) now operates to allow two international collaborations to use these techniques to pursue cold \bar{H} . ATRAP (which grew out of TRAP) demonstrated the crucial device and technique for producing cold antihydrogen about a year ago – the e^+ cooling of \bar{p} in a nested Penning trap [6]. It remains to show clearly that cold antihydrogen was being formed during ATRAP’s positron cooling of antiprotons in a nested Penning trap. Both ATRAP and ATHENA set about using this production method. Two reports by ATRAP [8,9] and one by ATHENA [7] confirmed that cold antihydrogen was made, using detection techniques that were quite different.

The observations of cold \bar{H} start an exciting time, though much remains to be done. \bar{H} atoms that are cold enough to be trapped for laser spectroscopy promise to provide the most stringent CPT tests with baryons and leptons [2], along with more sensitive tests for possible extensions to the standard model [10], building on the high accuracy of hydrogen spectroscopy [11]. It may even be possible to directly observe the gravitational force on antimatter atoms [12]. \bar{H} atoms with a temperature near to the 0.5 K depth of a realistic magnetic trap are required if atoms are to be trapped from a thermal distribution with a reasonable efficiency.

2. ATRAP’s e^+ cooling of \bar{p} in a nested penning trap produces cold \bar{H}

The crucial step of demonstrating a way to produce cold \bar{H} was reported about a year ago when our ATRAP Collaboration demonstrated the first e^+ cooling of \bar{p} within a nested Penning trap [6]. The report suggested that near the end of the e^+ cooling process the slow passage of \bar{p}

through the e^+ plasma made it likely that \bar{H} was produced. Indeed it was, as indicated by the recent reports of observed \bar{H} by ATHENA [7] and ATRAP [8,9].

The key device allowing \bar{H} production is the nested Penning trap (Fig. 1) which we proposed long ago [13] as a way to allow e^+ and \bar{p} to interact while stored, despite the opposite sign of charge which keeps them from being confined together in the same Penning trap well. The e^+ are stored within a small inverted well at the center of a larger well for \bar{p} . The nested Penning trap is designed for the attainment of a cold, dense e^+ plasma and the slow passage of antiprotons through it, general conditions that favor \bar{H} production via well-known recombination mechanisms in plasmas [13]. Before using it to observe the e^+ cooling of \bar{p} , we investigated the nested Penning trap with e^- and p [14], and loaded cold \bar{p} and e^+ together within such a trap [15].

The key process for \bar{H} production is the e^+ cooling of \bar{p} in the nested Penning trap, since this cooling produces \bar{p} and e^+ with a low relative velocity limited by the thermal motions of the e^+ plasma, the condition under which \bar{H} production is expected to be optimal. The \bar{p} start with high enough energies to take them back and forth across the whole width of their well. They lose energy via collisions while passing through the e^+ plasma, which in turn radiates the transferred energy in the cyclotron motions of the e^+ (orders of magnitude faster than in those of the \bar{p}). The cooling becomes more efficient as the \bar{p} energy reduces to near where the \bar{p} and e^+ energies coincide and the two species have low relative velocities. The long interaction time that results is desired for efficient \bar{H} production.

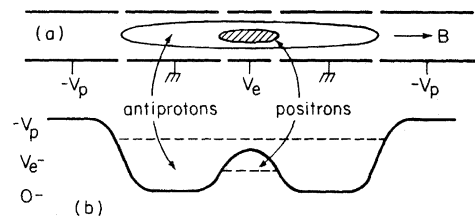


Fig. 1. Nested Penning trap allows positrons and antiprotons to interact at low relative velocity (from [13]).

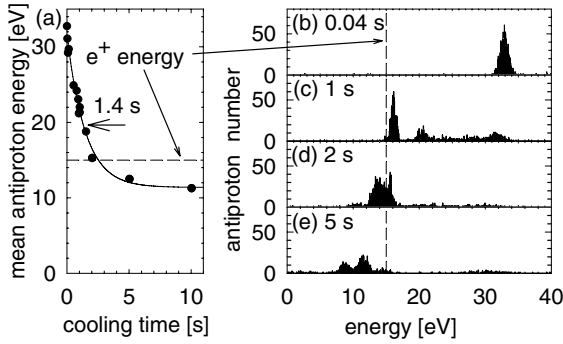


Fig. 2. (a) Antiproton average energy decreases exponentially in time until the \bar{p} and e^+ have the lowest relative velocity. Cooling then continues but at a 10 times slower rate. (b)–(e) Energy spectra of the \bar{p} as a function of the positron cooling time. (Here 5000 \bar{p} are used, along with 200,000 e^+ in a 15 V well, from [8].)

Fig. 2(a) shows an example of the energy of \bar{p} in a nested Penning trap decreasing exponentially as a result of collisions with cold e^+ . The \bar{p} energy spectra at a sequence of cooling times (Fig. 2(b)–(e)) reveal intricate structure, not yet completely understood. \bar{H} presumably forms near to where the energies of the \bar{p} (histograms) and e^+ (vertical dashed line) overlap, where the relative velocities are low.

On a 10 times longer time scale, we have also observed that the \bar{p} cool into the side wells of the nested trap, decreasing the interaction with the e^+ . The new cooling mechanism here seems to be a recycled evaporative cooling of the \bar{p} , whereby hot \bar{p} that “evaporate” to higher energies in the nested well are cooled by the e^+ before they can leave the well. With no e^+ in the nested well, evaporative cooling cools the \bar{p} on the slower time scale.

3. Observations of \bar{p} losses from a nested penning trap

Having first demonstrated e^+ cooling, ATRAP carefully studied \bar{p} losses from the nested Penning trap, and various intriguing signals that seemed related to \bar{H} production. \bar{H} is expected to form when e^+ cooling reduces the energy of \bar{p} to the point where the \bar{p} pass slowly through the e^+ plasma confined in the central well. Being neutral, \bar{H} will be free to drift out of the nested Penning

trap unless it is ionized on the way out. A resulting \bar{p} loss from the nested Penning trap is highly desirable if this loss is clearly due to \bar{H} formation.

Unfortunately, we have observed \bar{p} annihilations even when no e^+ are present in the nested Penning trap. Such losses occur when the \bar{p} energy is near the vertex of the inverted e^+ well in the center of the nested Penning trap, and do not occur when the \bar{p} energy is high enough above the vertex. Our detectors revealed that these \bar{p} were leaving the trap along radial directions perpendicular to the magnetic field. It is possible that such losses might be increased when e^+ are in the nested Penning trap. The \bar{p} loss was also observed with e^+ in the nested well. The e^+ cooling, however, accelerates the appearance of \bar{p} loss by quickly reducing the \bar{p} energy to the neighborhood of the inverted e^+ well where the losses occur.

Fig. 3 shows an example of \bar{p} loss when \bar{p} are repeatedly driven into collision with the e^+ plasma. The observed \bar{p} loss rate can be as high as 2000 \bar{p} /s, orders of magnitude larger than any claimed antihydrogen production rate, a disturbing evidence of \bar{p} transport mechanism/s during positron cooling. Observation of \bar{p} annihilations with the presence of e^+ , or of the reduced \bar{p} annihilations with increasing temperature of the e^+ plasma, is not a safe indication of antihydrogen production in view of such \bar{p} losses. Some way is needed to distinguish the two processes. The inadequacy of such a no-positrons control experiment kept us at ATRAP from claiming the observation of cold \bar{H} using this technique, despite our observation that e^+ in the nested Penning trap increased the number of coincident annihilations of \bar{p} and e^+ [17]. It seemed important to understand the \bar{p} losses well enough to ensure that observations of cold \bar{H} were not

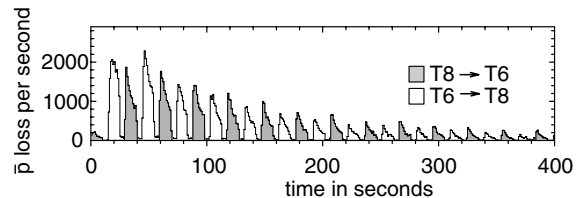


Fig. 3. Antiprotons lost while being driven from one side of the nested Penning trap (T6) to the other (T8). The e^+ plasma is confined in the central well T7 (from [9]).

instead due to \bar{p} loss induced by e^+ cooling without \bar{H} formation.

4. Detection of \bar{H} using coincident annihilation of \bar{p} and e^+

If \bar{p} loss by itself does not indicate the production of \bar{H} , one might expect that a simultaneous annihilation of an e^+ and a \bar{p} annihilation would unambiguously demonstrate that an \bar{H} atom was formed. Cold \bar{H} formed in the nested Penning trap will leave the trap and hit its electrodes, whereupon both the \bar{p} and e^+ will annihilate. The charged pions from \bar{p} annihilation can be detected with high efficiency with scintillators, scintillating fibers, or silicon strips. The 0.5 MeV gammas from e^+ annihilation can be detected using CsI or BGO detectors.

In practice, this method unavoidably has a background of false \bar{H} events which cannot be distinguished from real \bar{H} events. The detector resolution limits how accurately the relative position and time of \bar{p} and e^+ can be determined. One concern is that the ambipolar diffusion mechanism [16] could make unbound e^+ and \bar{p} correlate enough to diffuse out of the trap, perhaps even generating simultaneous annihilation of \bar{p} and e^+ . Another is that some \bar{p} annihilation branches generate secondary e^+ ; \bar{p} annihilation alone can produce a coincident e^+ annihilation. Clean, event-by-event identification of \bar{H} is not possible. Some way of estimating the number of true and false signals is thus needed before some of the annihilation signals can be attributed to cold \bar{H} .

At ATRAP we tried coincident annihilation detection, though with less axial and energy resolution than in the ATHENA detector [17]. The \bar{p} annihilations were detected in scintillators and scintillating fibers, and e^+ annihilations were detected in 12 BGO crystals that surrounded the nested Penning trap. Signals remained after subtracting what was seen with no e^+ in the nested Penning trap. As already mentioned, our careful studies of e^+ cooling in the nested Penning trap made us uncomfortable relying upon a no-positron control. Instead a different method was developed.

5. ATRAP's field ionization method

Concerns about the validity of no-positron controls, and the substantial background that cannot be avoided in coincident annihilation detection, prompted ATRAP to develop a field ionization method that avoids these difficulties. ATRAP was able to make a background-free observation of cold \bar{H} by field ionizing cold \bar{H} and storing the released \bar{p} until the e^+ cooling and its associated background were over [8]. A second ATRAP report demonstrated a method of driving the production of cold \bar{H} to further increase the production efficiency [9]. Much larger numbers of \bar{H} were observed per unit time and per high energy \bar{p} than has been seen to date – more \bar{H} being observed in an hour than the sum all reported earlier. The field ionization method also made it possible to measure the first distribution of \bar{H} states, giving the first glimpse inside the \bar{H} atom. Knowing the internal state of the \bar{H} is essential if methods to deexcite it to states useful for spectroscopy and trapping are to be developed.

For the demonstration of background-free observation of cold \bar{H} [8], ATRAP typically used 150,000 \bar{p} suspended within electrode T2 (Fig. 4(a)) and up to 1.7 million cold e^+ in electrode T5. To start e^+ cooling and \bar{H} formation, the \bar{p} are launched into the nested Penning trap by pulsing from the solid to the dashed potential (Fig. 4(b))

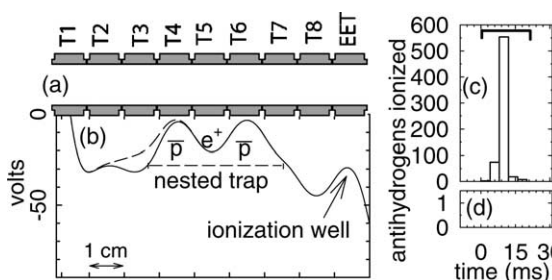


Fig. 4. (a) Electrodes for the nested Penning trap have an inner diameter of 1.2 cm. (b) The potential on axis for positron-cooling of antiprotons (solid) during which \bar{H} formation takes place, with the (dashed) modification used to launch \bar{p} into the well. (c) Antiprotons from \bar{H} ionization are released from the ionization well during a 20 ms time window. (d) No background \bar{p} are counted when no e^+ are in the nested Penning trap (from [8]).

for 1.5 μs . The \bar{p} oscillate back and forth within a nearly symmetrical nested Penning trap, restored before the \bar{p} return to their launch point. They lose energy via collisions as they pass through the e^+ , which cool via synchrotron radiation to the 4.2 K of their surroundings.

Any \bar{H} atom formed is free move in the direction of its \bar{p} , unconfined by the Penning trap. \bar{H} atoms passing through the field-ionization well in a state that can be ionized by the electric field, will leave their \bar{p} trapped in this well.

The ionization (or detection) well (within electrode EET in Fig. 4(a)) is carefully constructed so that its electric field ensures that no \bar{p} from the nested Penning trap can get into it (e.g. a \bar{p} liberated from the nested well by ambipolar diffusion) except if it travels about 4 cm bound within an \bar{H} atom. Any \bar{p} heated out of the nested Penning trap escapes over the lower potential barrier in the other direction. Even if a \bar{p} did acquire enough energy to go over the ionization well in one pass it would not be trapped because there is no mechanism to lower its energy while over this well. Finally, in the crucial stages, e^+ cooling lowers the energy of the \bar{p} in the nested well, taking them further from the energy required to even pass over the ionization well.

Only signals from \bar{H} are detected with this field-ionization method – there is no background at all! Fig. 4(c) represents 657 ionized \bar{H} captured in the ionization well during the course of this experiment – more than all the \bar{H} atoms reported so far. In many trials without e^+ we have never seen a single \bar{p} in the ionization well (Fig. 4(d)). Antiprotons from \bar{H} ionization are stored in the ionization well until after positron cooling is completed in the nested well, and all other \bar{p} and e^+ are released in the direction away from the ionization well. We then eject the stored \bar{p} by ramping down the potential of the ionization well in 20 ms. The ejected \bar{p} annihilate upon striking electrodes, generating pions and other charged particles that produce light pulses in the scintillators. The ramp is fast enough so that the 1.2/s cosmic ray background contributes a count in our window only one time in 50 in Fig. 4(b)–(c). Our experimentally calibrated detection efficiency corresponds to 1 in 2.7 of the stored \bar{p} producing a coincidence signal in surrounding scintillators.

The number of ionized \bar{H} atoms increases with the number of e^+ in the nested well (Fig. 5(a)) as might be expected, though this curve is surprisingly insensitive to the total number of e^+ for larger e^+ number. We are exploring some indications that the shape of this measured curve is related to a quadratic dependence of the production rate upon e^+ density. The ionization well can be moved further away from the center of the nested well, using identical electrodes to the right of EET in Fig. 4(a). The decrease in the number of ionized \bar{H} (Fig. 5(b)) seems consistent with a quadratic dependence on distance, showing that the \bar{H} angular distribution is broader than the small solid angle subtended by our ionization well. Isotropic \bar{H} production and a broad \bar{H} “beam” along the direction of the magnetic field are both consistent with Fig. 5(b). More study is needed to estimate carefully how much the trajectories of the highly polarizable Rydberg atoms are modified by the electric and magnetic fields.

Ionization of \bar{H} produced during e^+ cooling of \bar{p} in a nested Penning trap has interesting consequences. For example, charge capture (recombination) causes reheating of \bar{p} insofar as \bar{H} formed are later ionized by the fields of a nested Penning trap, which recaptures their \bar{p} at higher energies. Furthermore, charge capture (recombination) causes radial transport of \bar{p} insofar as \bar{H} formed move out radially before they are ionized by the

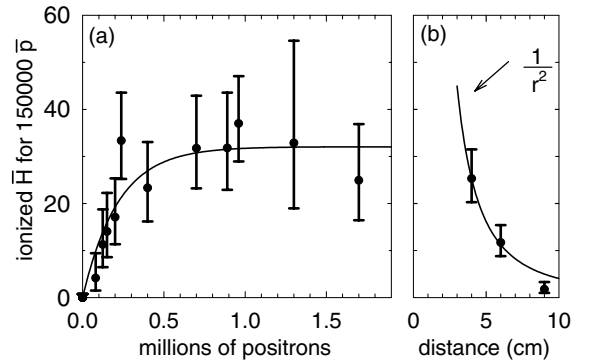


Fig. 5. (a) The number of field-ionized \bar{H} increases with the number of e^+ in the nested Penning trap of Fig. 4, and then levels off. (b) This number decreases when the ionization well is moved away from the nested Penning trap (from [8]).

fields of a nested Penning trap, which recaptures their \bar{p} at larger radii – even beyond the e^+ plasma radius. The dynamics in a nested Penning trap is greatly enriched by such ionization effects. It is important to study such processes in a nested Penning trap, which are relevant to measurements of cross-sections and stopping powers, for example.

To give some idea of how efficiently \bar{H} atoms are stripped and detected we use one trial in which eight AD injection pulses are used to accumulate 148,000 cold \bar{p} , 430,000 cold e^+ accumulate simultaneously. After the positron cooling of the antiprotons we determine that 66 \bar{H} have field ionized and left their \bar{p} in the ionization well. This means that we observe about eight \bar{H} atoms per AD injection pulse, and about 1 \bar{H} atom per 2200 \bar{p} in the nested well.

If the \bar{H} production at ATRAP is isotropic, then the 657 ionized \bar{H} would represent nearly 170,000 cold \bar{H} . This would mean that a remarkable 11% of the \bar{p} in the nested Penning trap are forming \bar{H} atoms – comprising a substantial portion of the large \bar{p} losses we have been observing during positron-cooling of antiprotons since this cooling was first observed. (The ionization well covers only about 1/260 of the total solid angle.)

6. Driven \bar{H} production and the first measured distribution of \bar{H} states

Knowledge of the \bar{H} states produced is required to devise methods to prepare states useful for trapping and precision spectroscopy. In the second ATRAP observation [9], a distribution of \bar{H} states is measured for the first time, for a high \bar{H} production rate realized by driving \bar{p} into collisions with cold e^+ .

This time the \bar{H} states are analyzed as they pass through an electric field that is varied without changing the separated \bar{H} production and detection. The \bar{p} are resonantly driven through trapped e^+ , back and forth from one side of a nested Penning trap to the other, in a new and efficient \bar{H} production method. \bar{H} forms during the e^+ cooling of \bar{p} over many cycles, until most of the trapped \bar{p} have formed \bar{H} , or are otherwise lost from the trap. A higher \bar{H} production rate, per \bar{p} coming to

our apparatus, compensates for the reduced detection solid angle resulting from the clean spatial separation of production and detection. The high rate and observed Rydberg states is what would be expected for a three body recombination mechanism [13,18,19].

For this observation, the nested Penning trap [6,13–15] is again central to \bar{H} production (Fig. 6(a)–(b)). Typically 300,000 cold e^+ are in the central inverted well, with typically 200,000 \bar{p} either divided between the two sides of the nested Penning trap (within T6 and T8), or placed in one side well.

The ionization and normalization wells (Fig. 6(a)–(c)), to the right and left of the nested Penning trap, are both designed to prevent \bar{p} not bound in \bar{H} from being captured. A \bar{p} heated out of the nested Penning trap will escape over the normalization well, unless there is a mechanism to lower the \bar{p} energy within this well. To make this harder we keep the potential on the left of this well lower by 3 V (on axis) than that of its right side. Getting a \bar{p} into the ionization well not only requires an energy loss within the well, but also requires that the \bar{p} climb a substantial potential barrier. Positron cooling keeps the \bar{p} from being heated, making it less likely that \bar{p} will be able to pass through the ionization and normalization wells when e^+ are in the nested well.

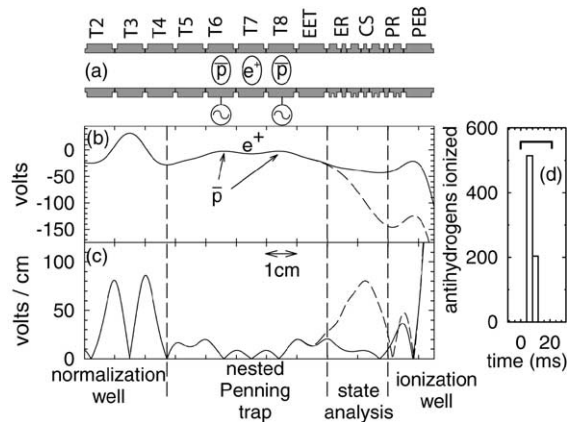


Fig. 6. (a) Trap electrodes, (b) potential on axis, (c) two values of the electric field magnitude on axis, (d) in a 1 h trial 718 \bar{p} from \bar{H} were captured in the ionization well (from [9]).

Electric fields within the ionization and normalization wells are made large to ionize \bar{H} passing through and capture their \bar{p} . Fig. 6(a) shows the electric field on the trap axis; in the critical state-analysis region, it varies by only about 10% off the axis. Numerical modelling of \bar{H} paths reveals that \bar{H} stripped by a field between 25 and 150 V/cm leave \bar{p} in the ionization well, while \bar{H} stripped between 35 and 140 V/cm deposit \bar{p} in the normalization well.

\bar{H} state analysis, a central feature of this work, is done by varying the potential offset between the nested and ionization wells. This varies the state-analyzing field that \bar{H} encounter on their way to the ionization well, as illustrated by two examples in Fig. 6(c). Any \bar{H} stripped by this field is unable to deposit its \bar{p} in the ionization well, causing the measured number of \bar{p} in this well, N , to decrease. (The stripping field in this well is stronger than are the state-analysis fields.) The number N_{norm} of \bar{p} from \bar{H} ionization in the normalization well provides a normalization.

Crucial radiofrequency drive potentials (1 V peak-to-peak at 825 kHz) applied alternatively to electrodes T6 or T8 (Fig. 6(a)) drive \bar{p} between the sides of the nested Penning trap. During each cycle, e^+ cooling allows the \bar{p} to settle into the opposite, undriven side well of the nested Penning trap, and some form \bar{H} during this cooling. Some optimization of the drive frequency and amplitude was done, but most of a large parameter space remains to be explored.

We alternately drive \bar{p} in one side then the other of the nested well for 10 s, with 5 s between, up to 25 times. Typically we transfer most \bar{p} from one side to the other, though asymmetries make it common for a constant remnant of a few ten thousands of \bar{p} to remain in one side well during the whole sequence. The drive cycle timing was not optimized.

To detect \bar{p} deposited in the ionization and normalization wells from \bar{H} ionization, we ramp down these potential wells in 20 ms, after the driving and associated particle loss are over, just as described before. Fig. 6(d) represents a background-free observation of 718 \bar{p} captured in an ionization well from \bar{H} ionization in a single, 1-h trial. With no e^+ in the nested well no \bar{p} from \bar{H} ionization are detected.

The observed \bar{H} production rate, per \bar{p} and per detection solid angle, is up to a factor of 12 greater than that observed using one-time positron cooling of antiprotons [8]. The \bar{H} rate seems very sensitive to the number of e^+ in the nested well, unlike the results for the one-time cooling. This makes some sense insofar as the driving process continually heats the \bar{p} and hence the e^+ they collide with. More e^+ would transfer this heat more rapidly into synchrotron radiation, and increase \bar{p} and e^+ overlap. Here again much parameter space remains to be explored. We presume that the \bar{H} are cold, insofar as the \bar{H} is likely made after very effective e^+ cooling of \bar{p} , but this must also be checked.

The first measured distribution of \bar{H} states is displayed in Fig. 7(a). The ratio (R), of the number of \bar{p} from \bar{H} stripped in the ionization well (N) to the corresponding number in the normalization well (N_{norm}), is plotted as a function of the state-analysis field (F). The number of \bar{H} that survive this field decreases linearly until consistent with zero. The error bars prevent seeing curvature near this point, so we use simple linear dependence

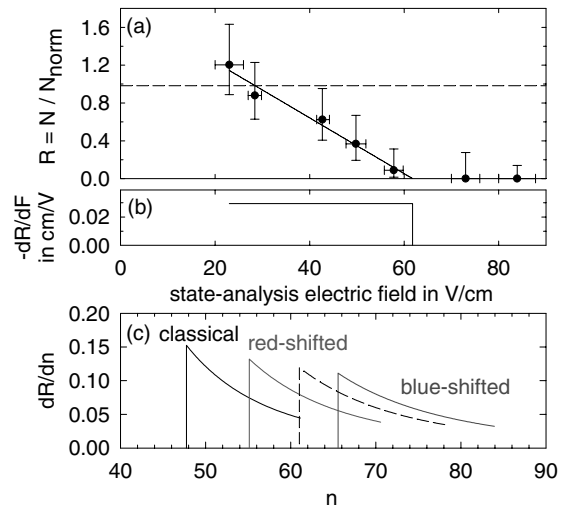


Fig. 7. (a) The ratio of ionized \bar{H} in ionization and normalization wells decreases linearly with state-analysis electric field F . (b) Distribution dR/dF is flat up to a cutoff. (c) State distributions dR/dn extracted from measured field distribution (b) using some classical and quantal models that relate F and n (from [9]).

going to zero to explore principal features. Thus dR/dF (Fig. 7(b)) is constant up to a cutoff. As many \bar{H} states are ionized by fields between 30 and 35 V/cm as between 55 and 60 V/cm, for example. No observed \bar{H} states require a stripping field greater than 62 V/cm.

It would be more satisfying to characterize the distribution of \bar{H} excited states by their principle quantum number n , rather than by the electric field that strips them. The first difficulty is that n is not a good quantum number in the strong magnetic field, though we still use n as a rough parameterization of binding energy, using $E = -13.6 \text{ eV}/n^2$. Ionization likely takes place in the direction of the magnetic field [20], giving some hope that it may not be strongly modified by the magnetic field, but this must be investigated.

The second difficulty is that the types of states formed determine the electric field that will ionize them, even in the absence of any magnetic field, as is well known from studies of the ionization of Rydberg atoms [21]. Fig. 7(c) shows n distribution for various models, which we have described in more detail [9]. Fortunately, classical and quantum calculations are underway.

Further enhancements of \bar{H} production might be possible with optimizations and variations on our method of arranging for many cycles of positron cooling of antiprotons. One might be to simultaneously drive \bar{p} on both sides of the nested Penning trap. Another would be to lift \bar{p} from the bottom of the nested well in a potential “bucket” for launching back into the nested Penning trap.

7. Conclusions and acknowledgements

In conclusion, ATRAP’s positron cooling of cold antiprotons [6] produces cold antihydrogen. ATHENA [7] and ATRAP [8,9] both report the production of cold \bar{H} using this device and technique. The observed \bar{H} production is encouragingly high, especially when we drive the \bar{p} into collisions with e^+ in a nested Penning trap.

ATRAP’s field ionization method allows a background-free observation of cold antihydrogen. It also allowed ATRAP to measure the first distribution of \bar{H} states using a pre-stripping electric

field in a separate region between where the \bar{H} are produced and detected. The observed distribution appears to be constant as a function of the state-analysis field, up to cutoff. The Rydberg states and high production rate are consistent with a three-body recombination mechanism and its deexcitation processes due to collisions [13,18,19].

The high production rate and measured state distribution give hope that it may be possible to devise a new way to deexcite Rydberg atoms with a range of binding energies and still get enough atoms for trapping and spectroscopy. Some temporary confinement of these highly polarizable states may be possible, but conventional trapping awaits deexcitation to the ground state, whereupon a goal is to superimpose a magnetic trap for \bar{H} with the Penning traps needed for its \bar{p} and e^+ ingredients [22]. The ATRAP field ionization method can be extended to more deeply bound states by increasing the size of the electric field. For states not accessible in this way, an excitation laser can be used to excite the deeply bound states to where they can be ionized and stored in the same way.

Thanks to CERN, its PS Division and the AD team for delivering 5.3 MeV antiprotons. ATRAP is supported by the NSF, AFOSR, the ONR of the US, the BMBF, MPG and FZ-J of Germany, and the NSERC, CRC and PREA of Canada.

References

- [1] G. Gabrielse, in: P. Bloch, P. Paulopoulos, R. Klapisch (Eds.), *Fundamental Symmetries*, Plenum, New York, 1987, p. 59.
- [2] G. Gabrielse, *Adv. Atomic Mol. Opt. Phys.* 45 (2001) 1.
- [3] G. Gabrielse, N.S. Bowden, P. Oxley, A. Speck, C.H. Storry, J.N. Tan, M. Wessels, D. Grzonka, W. Oelert, G. Schepers, T. Sefzick, J. Walz, H. Pittner, T.W. Hänsch, E.A. Hessels, *Phys. Lett. B* 548 (2002) 140.
- [4] G. Baur et al., *Phys. Lett. B* 368 (1996) 251.
- [5] G. Blanford, D.C. Christian, K. Gollwitzer, M. Mandelkern, C.T. Munger, J. Schulz, G. Zioulas, *Phys. Rev. Lett.* 80 (1998) 3037.
- [6] G. Gabrielse, J. Estrada, J.N. Tan, P. Yesley, N.S. Bowden, P. Oxley, T. Roach, C.H. Storry, M. Wessels, J. Tan, D. Grzonka, W. Oelert, G. Schepers, T. Sefzick, W. Breunlich, M. Carnielli, H. Fuhrmann, R. King, R. Ursin, H. Zmeskal, H. Kalinowsky, C. Wesdorp, J. Walz, K.S.E. Eikema, T.W. Hänsch, *Phys. Lett. B* 507 (2001) 1.

- [7] M. Amoretti et al., *Nature* 419 (2002) 456.
- [8] G. Gabrielse, N.S. Bowden, P. Oxley, A. Speck, C.H. Storry, J.N. Tan, M. Wessels, D. Grzonka, W. Oelert, G. Schepers, T. Sefzick, J. Walz, H. Pittner, T.W. Hänsch, E.A. Hessels, *Phys. Rev. Lett.* 89 (2002) 213401.
- [9] G. Gabrielse, N.S. Bowden, P. Oxley, A. Speck, C.H. Storry, J.N. Tan, M. Wessels, D. Grzonka, W. Oelert, G. Schepers, T. Sefzick, J. Walz, H. Pittner, T.W. Hänsch, E.A. Hessels, *Phys. Rev. Lett.* 89 (2002) 233401.
- [10] R. Bluhm, V.A. Kostelecký, N. Russell, *Phys. Rev. D* 57 (1998) 3932.
- [11] M. Niering, R. Holzwarth, J. Reichert, P. Pokasov, T. Udem, M. Weitz, T.W. Hänsch, P. Lemonde, G. Santarelli, M. Abgrall, P. Laurent, C. Salomon, et al., *Phys. Rev. Lett.* 84 (2000) 5496.
- [12] G. Gabrielse, *Hyperfine Interact.* 44 (1988) 349.
- [13] G. Gabrielse, S.L. Rolston, L. Haarsma, W. Kells, *Phys. Lett. A* 129 (1988) 38.
- [14] D.S. Hall, G. Gabrielse, *Phys. Rev. Lett.* 77 (1996) 1962.
- [15] G. Gabrielse, D.S. Hall, T. Roach, P. Yesley, A. Khabbaz, J. Estrada, C. Heimann, H. Kalinowsky, *Phys. Lett. B* 455 (1999) 311.
- [16] R.J. Goldston, P.H. Rutherford, *Introduction to Plasma Physics*, Inst. of Phys, London, 1995.
- [17] To be published.
- [18] M. Glinsky, T. O'Neil, *Phys. Fluids B* 3 (1991) 1279.
- [19] P.O. Fedichev, *Phys. Lett. A* 226 (1997) 289.
- [20] W. Ihra, F. Mota-Furtado, P.F. O'Mahony, *Phys. Rev. A* 58 (1998) 3884.
- [21] T.F. Gallagher, *Rydberg Atoms*, Cambridge University Press, New York, 1994.
- [22] T.M. Squires, P. Yesley, G. Gabrielse, *Phys. Rev. Lett.* 86 (2001) 5266.